

Forced Sahel rainfall trends in the CMIP5 archive

Michela Biasutti

Abstract. The simulations of the fifth Coupled Models Intercomparison Project (CMIP5) strengthen previous assessments of a substantial role of anthropogenic emissions in driving precipitation changes in the Sahel, the semi-arid region at the southern edge of the Sahara. Historical simulations can capture the magnitude of the centennial Sahel drying over the span of the 20th century and confirm that anthropogenic forcings have contributed substantially to it. Yet, the models do not reproduce the amplitude of observed oscillations at multi-decadal time scales, suggesting that either oscillations in the forcing or the strength of natural variability are underestimated. Projections for Sahel rainfall are less robust than the 20th century hindcast and outlier projections persist, but overall the CMIP5 models confirm the CMIP3 results in many details and reaffirm the prediction of a rainy season that is more feeble at its start, especially in West Africa, and more abundant at its core across the entire Sahel. Out of 20 models, 4 buck this consensus. Idealized simulations from a sub-set of the CMIP5 ensemble—simulations designed to separate the fast land-atmosphere response to increased greenhouse gases from the slow response mediated through changes in sea surface temperature (SST)—confirm that the direct effect of CO₂ is to enhance the monsoon, while warmer SST induce drying over the Sahel. At the same time, these simulations suggest that the seasonal evolution of the rainfall trends in the scenario simulations, spring drying and fall wetting, is an inherently coupled response, not captured by the linear superposition of the fast and slow response to CO₂.

1. Introduction

Rainfall in the Sahel has experienced substantial multi-decadal swings and an overall reduction during the course of the 20th century (Figure 1). Paleoclimate records indicate that North Africa has suffered prolonged droughts before [Nicholson, 1978; Brooks, 1998; Shanahan *et al.*, 2009], but whether the remarkable drying of the Sahel over the course of the 20th century was natural or man-made is an open question. Recent pluvials and drought in the Sahel have been mostly controlled by concomitant variations in sea surface temperature [SST, for example Giannini *et al.*, 2003; Hagos and Cook, 2008], but the natural or anthropogenic origin of these is debated [e.g. Zhang *et al.*, 2006; Ting *et al.*, 2009; Mohino *et al.*, 2011; Booth *et al.*, 2012].

Biasutti and Giannini [2006] noted that the CMIP3 models reproduced a centennial drying in the Sahel and interpreted the consensus across models to indicate that anthropogenic forcing had caused about a third of the long-term 20th century drying. Ackerley *et al.* [2011] used a perturbed physics ensemble to come to a stronger conclusion: that most of the drying between 1940 and 1980 was due to anthropogenic reflective aerosols, via their influence on the SST gradient in the Atlantic. Yet, the strength of the indirect aerosol forcing is controversial [Stevens and Feingold, 2009], and dismissing a strong role for natural variability is premature [Ting *et al.*, 2009; Biasutti, 2011; Evan, 2012], especially at timescales less than a century, at which the influence of the Atlantic Multi-decadal Variability might be dominant [Hoerling *et al.*, 2006; Zhang *et al.*, 2006; Mohino *et al.*, 2011]. Similarly, the most recent recovery of the rains [Nicholson *et al.*, 2000] might be simply natural variability [Mohino *et al.*, 2011] or a forced response to increased greenhouse gases [GHGs Haarsma *et al.*, 2005] or reduced aerosols [Ackerley *et al.*, 2011]. Attribution is confounded by

the lack of consensus across the CMIP3 models on future trends in summertime rainfall [Held *et al.*, 2005; Cook and Vizy, 2006; Biasutti *et al.*, 2008]. The profound model biases in both climatology and modes of coupled rainfall/SST variability [for example, Cook and Vizy, 2006; Joly *et al.*, 2007] also limit our confidence in a quantitative attribution of the past drought to any one forcing and some studies have noted that SST alone is insufficient to force the full amplitude of Sahel variations in most uncoupled models [e.g. Scaife *et al.*, 2008] and that Sahel rainfall is sensitive to vegetation and dust processes that are not routinely included in coupled models [Zeng *et al.*, 1999; Yoshioka *et al.*, 2007; Kucharski *et al.*, 2012].

Here we show that the newest generation of coupled models, those participating in CMIP5, reaffirm the results of CMIP3. In particular, we find that historical simulations accurately capture the centennial drying trend, even as they fail to fully represent the multi-decadal oscillations. We also show that, while some uncertainty in future summertime projections persists in the CMIP5 ensemble, there is qualitative agreement with CMIP3 in both the pattern and the seasonal evolution of the rainfall anomalies. This agreement lends credence to the multi-model mean projection of a rainy season that starts out more feebly, but becomes more intense at its core and end. The CMIP5 suite of simulations comprises idealized runs that can distinguish the role of SST warming from the direct effect of CO₂ on the land-atmosphere climate; these are analyzed to understand the origin of the Sahel rainfall anomalies in scenario simulations.

2. Data

We use four sets of simulation from the CMIP5 archives [Taylor *et al.*, 2012]: pre-industrial, historical, scenario, and idealized simulations. Pre-industrial control simulations provide a baseline for the natural variability in the climate system, in the absence of any anthropogenic forcings. Historical simulations are forced by best estimates of historical natural forcings (e.g., volcanoes and solar irradiance)

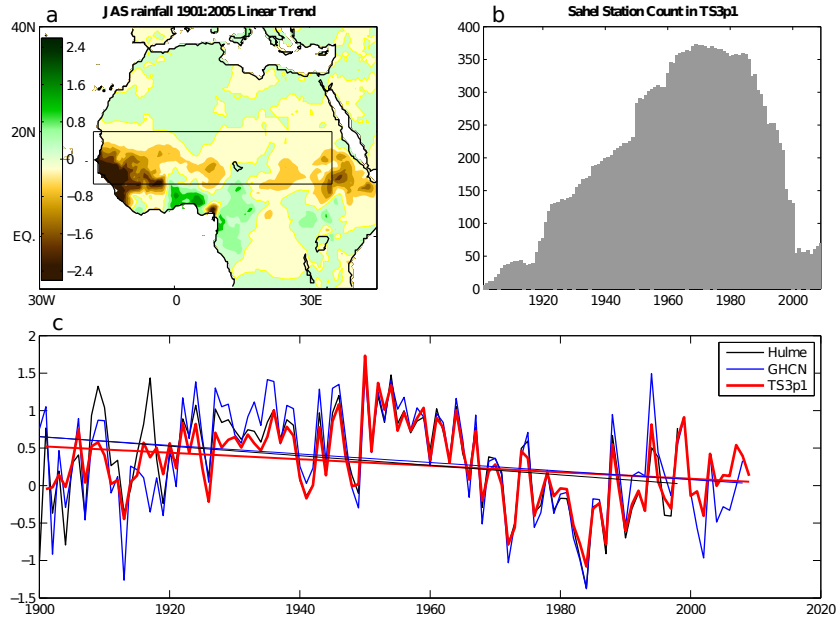


Figure 1. Observed rainfall trends in the Sahel. Top left (a): July-August-September rainfall trend in the TS3p1 dataset. Shading is in mm/day and is the difference between the end point of the linear trend over 105 years (1901:2005). The box indicates the Sahel. Top right (b): number of TS3p1stations inside the Sahel box as a function of time. Bottom (c): JAS Sahel rainfall in three observational datasets, plotted as anomalies from the 1979-1998 average, and linear trends over the span of the dataset; TS3p1 and Hulme are gridded products of the Climate Research Unit, while the Global Historical Climatology Network provides individual stations that are simply averaged across the Sahel, without any attempt at dealing with inhomogeneity in the coverage.

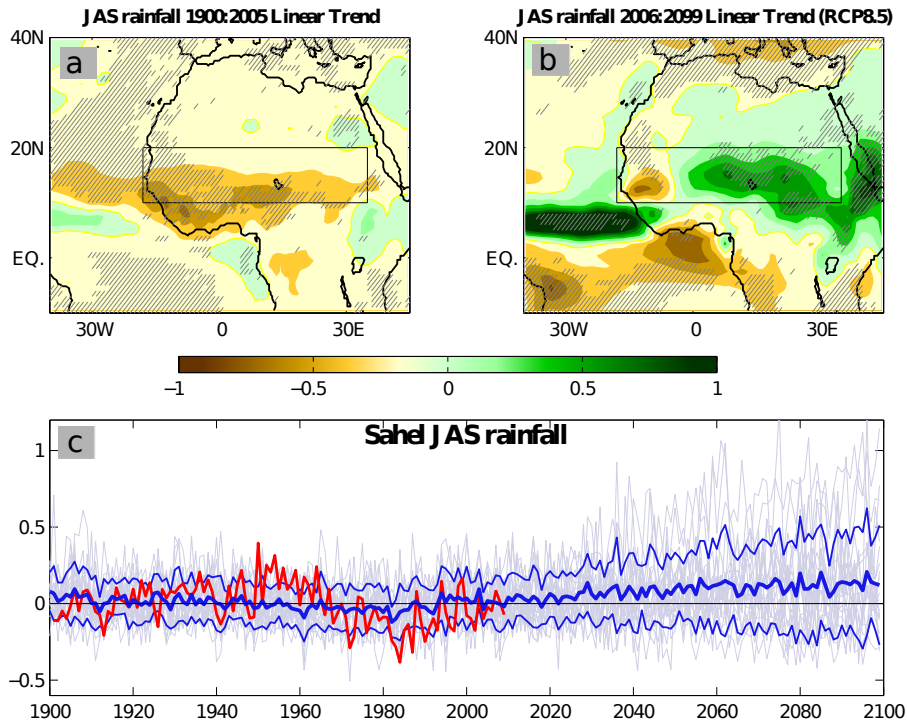


Figure 2. Top: Historical and RCP8.5 scenario trends in summertime rainfall. Maps are in mm/day and are the difference between the end point of the linear trend over 105 years (1900:2005, left) and 95 years (2006:2099, right). The mean of available ensemble runs is used for each model (using the 20 models that have both historical and RCP8.5 simulations). Stippling indicates grid boxes where 15 or more of the models produced either a positive or a negative trend. The boxes indicate the Sahel. Bottom: JAS Sahel rainfall in the models and observations. Light grey lines are individual model runs, the thick solid blue line is the multi-model mean, the thin blue lines indicate the one standard deviation spread, the red line is observations (TS3p1). The time series are in units of fraction of mean JAS rainfall, where the mean is taken over the 1900-1999 period for the models and over 1901-1999 for TS3p1).

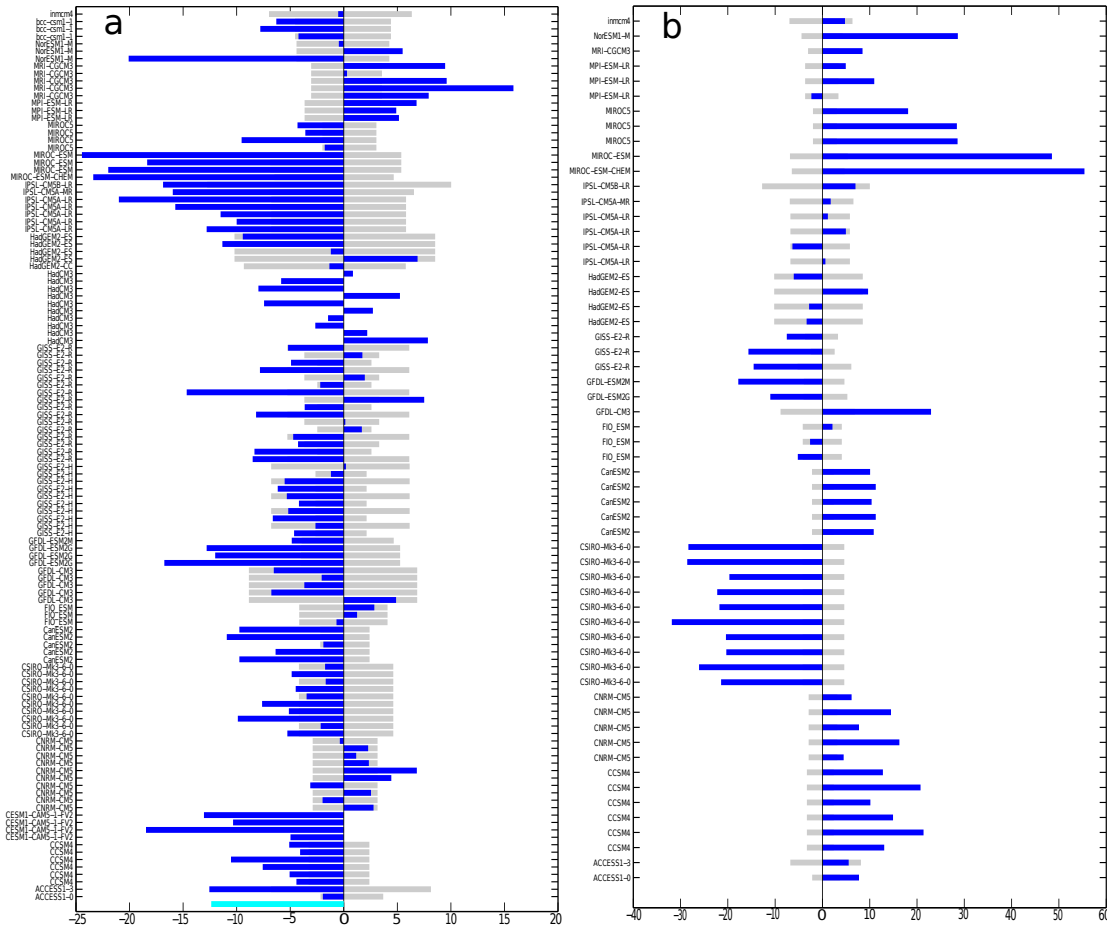


Figure 3. Centennial-scale trends in summertime Sahel rainfall. Trends during 1900:2005 (left) and 2006:2099 (right) in individual ensemble members and observations (Ts3p1, cyan bar in the left panel). Units are in percent of mean summer rainfall. The background gray shading shows the 1 standard deviation in trends over the same length of time in the corresponding pre-industrial control integrations.

cycle and atmospheric chemistry alongside simpler ocean-atmosphere coupled models, the concentration and distribution of radiatively active gases and aerosols are not the same in all historical simulations [Friedlingstein *et al.*, 2006]. Similarly, different treatments of the interaction of aerosols and clouds leads to different indirect aerosol forcing. We start our analysis of historical runs from 1900, when observations over Africa are available. The RCP8.5 scenario is used for the remainder of the 21st century, due to the greater number of available simulations. As described in Riahi *et al.* [2011], “RCP8.5 depicts a relatively conservative business as usual case with low income, high population and high energy demand due to only modest improvements in energy intensity”. This is an extreme scenario, with a continuous rise in radiative forcing during the 21st century, leading to a value of about 8.5 Wm^{-2} in 2100; such growth in radiative forcing is achieved mostly by a tripling of carbon emission within this century, while sulfate emissions are cut to a quarter. Emission scenarios for a number of other greenhouse gases and atmospheric pollutants, as well as estimates of future changes in land use, are also specified. Irrespective of how models treat chemically active species and the carbon cycle, the GHG forcing grows fast and dominates over the effect of aerosols by the end of the century [although the response to changes in aerosols are far from being negligible for regional climate, see Levy II *et al.*, 2008, 2012]. Idealized simulations that only include forcing from increasing CO2 concentrations (see section 4) supports the assumption that

GHGs effect much of the Sahel rainfall changes seen in the scenario simulations.

Two versions of the University of East Anglia Climate Research Unit gridded monthly precipitation datasets are used to assess trends in observations. The Hulme dataset [Hulme, 1992] covers 1900-1998 and TS3p1 [Mitchell and Jones, 2005] covers 1901-2009. The latter dataset optimizes for comprehensiveness and not stability, but the two sources agree well among themselves and with a simple arithmetic average of available stations from the Global Historical Climatological Network [Peterson and Vose, 1997, see Figure 1]. Of course, the observations going in any of these products are the same, so it is possible that all datasets are biased at the beginning of the century, when the station data is extremely scarce (Figure 1). One source of confidence in the observations comes, remarkably, from GCM simulations forced by the observed SST, which duplicate the observed record even in the early decades of the 20th century (Isaac Held, personal communication and figure posted on <http://www.gfdl.noaa.gov/isaac-held-homepage>).

3. Historical trends and projections.

Figure 2 shows summertime (July, August, September, JAS) mean rainfall trends over the historical and scenario runs in 20 models (when possible, a model is represented by the mean of its ensemble runs). Where three quarters or more of the models simulate changes of the same sign,

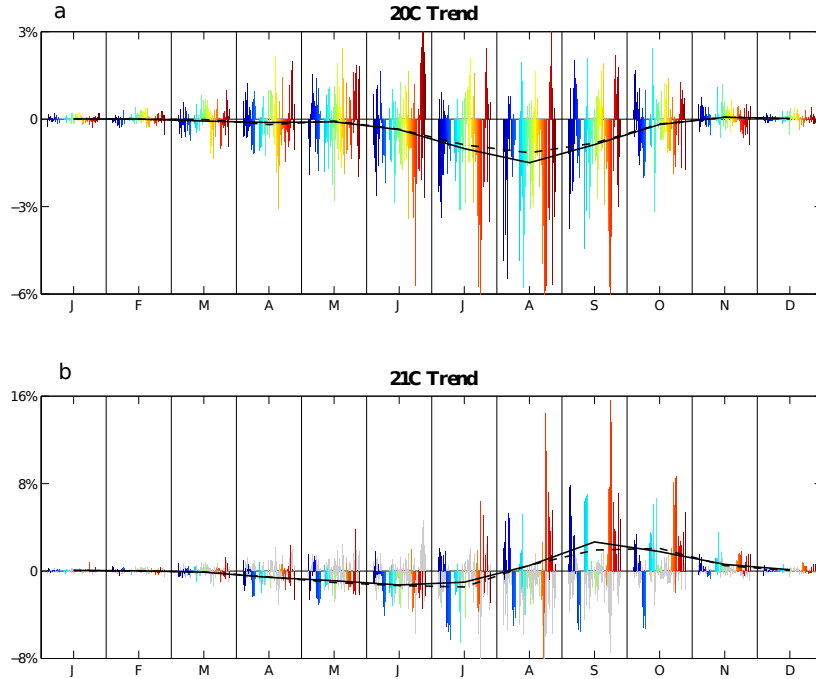


Figure 4. Annual cycle of Sahel rainfall trends. Historical (1900:2005, top) and RCP8.5 (2006:2099, bottom) trends in Sahel rainfall in single ensemble members for all calendar months. Units are in percentage of the long-term mean annual total rainfall. For reference, the historical trends are repeated as background gray bars in the bottom panel. The number of available simulations differs for the historical and scenario cases. The solid and dashed lines are the mean and median of the ensemble runs.

agreement across the ensemble is indicated by stippling. As did CMIP3, the CMIP5 ensemble captures the large scale drying of the entire Sahel during the 20th century both in the mean and in most individual models (Fig. 2a), although the drying pattern is displaced to the south compared to observations and much weaker than observed, especially on the mountains of Senegal. On average, the simulated Sahel rainfall index suggests little change before 1940, a rather linear drying between the 1940's and the 1980's, and a subsequent recovery (Fig. 2c). This progression matches observations quite well in a qualitative sense, but not in the magnitude of the interdecadal variations; in particular, neither the pluvial of the 1950s nor the severity of the drought in the 1970s and 1980s are captured in the multi-model mean. If internal multi-decadal variability of SST were the dominant cause for these oscillations [Ting *et al.*, 2009], the multi-model mean would not and should not capture them. On the other hand, the mismatch could be due to an underestimation of oscillations in the forcing, for example in the effect of aerosols [Ackerley *et al.*, 2011; Booth *et al.*, 2012]. One can find within the ensemble an individual integration matching observations, but in general most simulations underestimate the strength of the observed multi-decadal trends (see the discussion of Fig. 7 below).

Both the multi-model mean and a majority of models project a wetter Sahel everywhere but along the Atlantic coast (Fig. 2b). The inter-model agreement is significant enough to lend credence to the mean projection, but is not as good as in the historical simulation. This can be seen in the inter-model standard deviation for the Sahel index, which remains constant in the historical simulations but grows by two thirds by the end of the 21st century, indicating growing disagreement (Fig. 2c).

Disagreement in Sahel rainfall projections was present in CMIP3 and is yet to be fully explained; this was a true disagreement rather than an indication that anthropogenic trends in the region will be negligible [Power *et al.*, 2012]. It

should not surprise, then, that similar disagreements would surface in CMIP5 or even be amplified, given the additional uncertainty in the projected radiative forcings. When the individual model trends are shown against the typical range of comparable trends in the pre-industrial controls (Figure 3), they confirm that positive and negative projections are both significant. Thus, as in CMIP3, we do not predict negligible trends in the Sahel. Instead we see substantial, but opposite, responses in different models: half of the models show a clear wetting, a quarter show clear drying and the rest shows no significant trends. For comparison, only 2 out of 20 models project a significant wetting trend in the 20th century (see Figure 3 and Figure 7).

The disagreement across models is reduced, but not eliminated, in the months leading in and out of the rainy season. Biasutti *et al.* [2009] and Biasutti and Sobel [2009] had noticed that the seasonality of rainfall trends in the 20th and 21st centuries differed: while the drying trend of the past was consistent throughout the rainy season (in both observations and the CMIP3 models), the future projections were better interpreted as a delay in the rainy season, with negative trends in the onset months (June-July, JJ) and positive trends in the demise months (September-October, SO). The same seasonality is duplicated in CMIP5, as seen in the rainfall trends in each calendar month in the historical and scenario simulations (Figure 4). There is enough noise in these simulations that both positive and negative trends are simulated for all calendar months in both epochs. Yet it is clear that the 20th century is characterized by overall negative trends (mimicking the shape of the rainy season, the negative trends peak in August) while the 21st century sees qualitatively different trends in the first half of the year (negative anomalies peaking in June and July) than in the second half (positive anomalies peaking in September). The negative anomalies in JJ are comparable to those seen in the 20th century, while the positive anomalies in SO are much

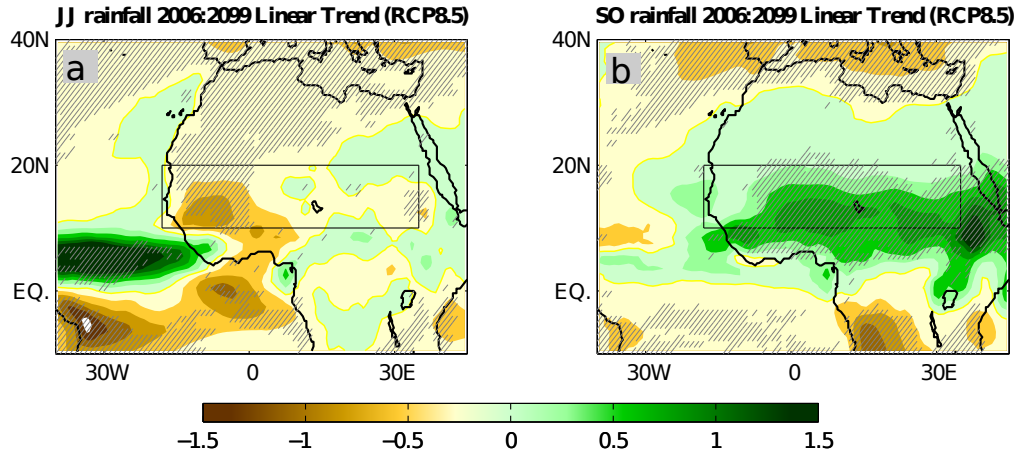


Figure 5. Rainfall projections for the onset and demise seasons. RCP8.5 trends in Sahel rainfall in the multi-model mean for the onset season (June and July, left) and the demise season (September and October, right). Maps are in mm/day and are the difference between the end point of the linear trend over 2006:2099. The mean of available ensemble runs is used for each model (using 20 models). Stippling indicates grid boxes where 15 or more of the models produced either a positive or a negative trend.

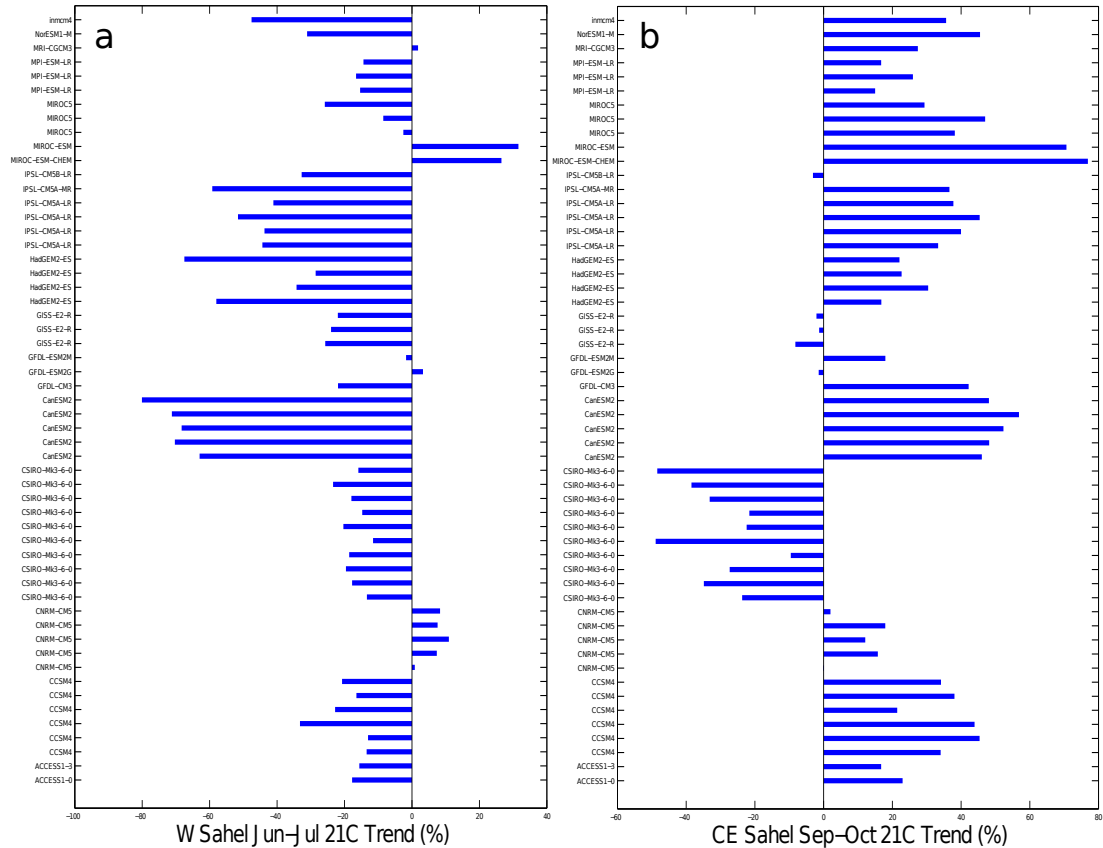


Figure 6. Centennial-scale trends in Sahel rainfall. Trends during 2006:2099 in individual ensemble members of the RCP8.5 simulations for June-July (left) and September-October (right) means in Western (left) and Central-Eastern Sahel (right), respectively. The two regions are to the west and east of 0W. Units are in percent of mean seasonal rainfall.

larger. The agreement in JJ and SO projections is still not as good as it was for summertime trends in the 20th century: the growing spread across models plotted in Figure 2 mars the onset and demise seasons as well (not shown), but this is ameliorated for sub-regions of the Sahel.

The difference in the spatial extent of the anomalies coming in and out of the rainy season is evident in Figure 5. The negative JJ anomalies are concentrated in West Africa, while the positive SO anomalies span the Sahel. When we define the West and Central-Eastern Sahel region to coincide with the regions of best agreement in the JJ and SO trend maps, we find that the sign of the centennial trends is

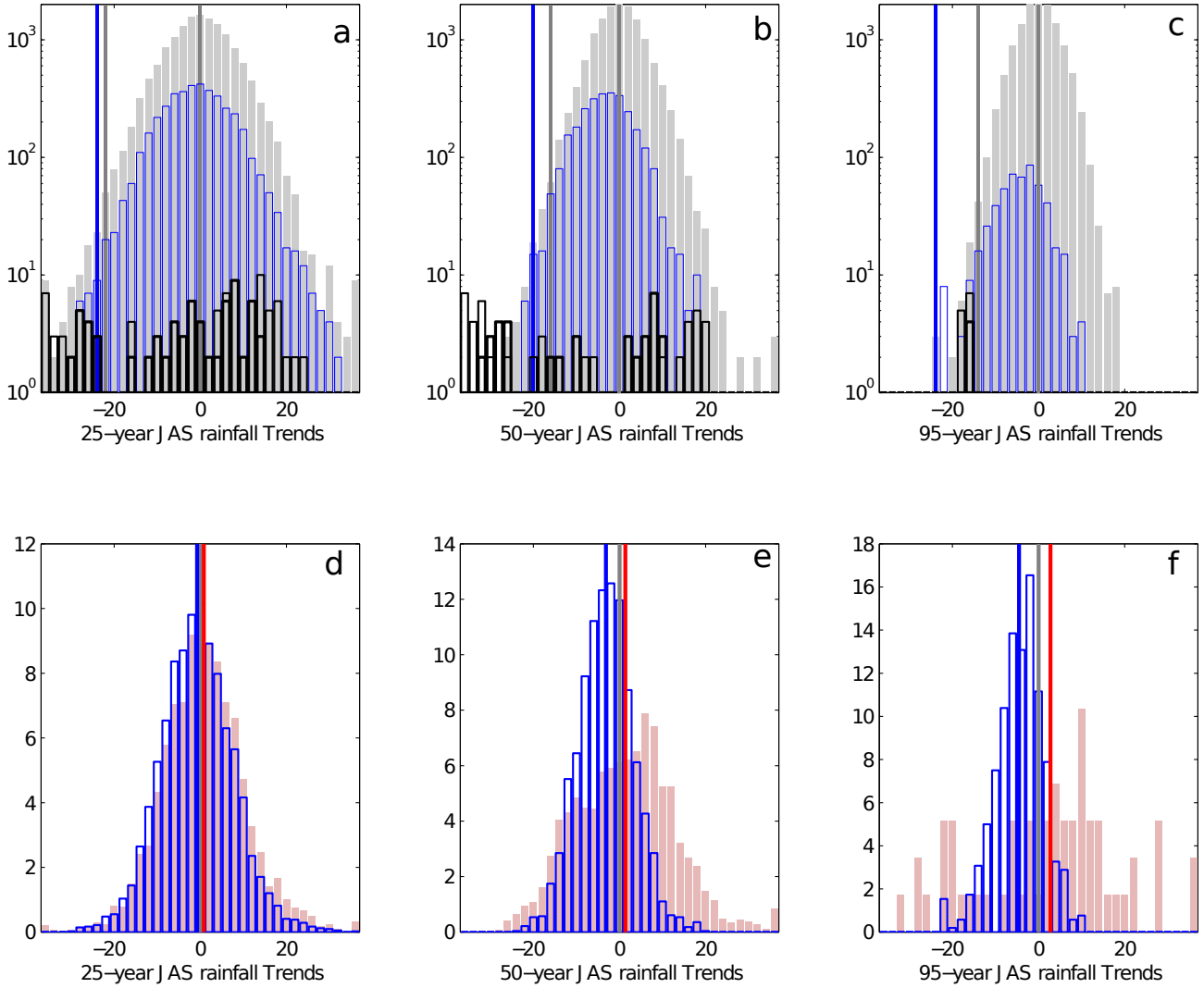


Figure 7. Character of simulated and observed trends in Sahel summer rainfall in different epochs. Distributions of 25-year (left), 50-year (center) and 95-year (right) trends in pre-industrial (gray, top), historical (blue, top and bottom), and RCP8.5 (red, bottom) integrations and in the observations (black, top; thicker line is for the Hulme dataset, thinner line for TS3p1). Histograms are not normalized in the top row and are plotted on a semi-log scale, while they are normalized and plotted on a linear scale in the bottom row. The vertical lines in the top panels indicate the one-in-a-hundred trends in the pre-industrial (gray) and historical (blue) ensembles. The vertical lines in the bottom row indicate the mean value of the trends in the historical (blue) and RCP8.5 (red) simulations. The zero value is also highlighted by a vertical gray bar in all panels.

quite robust (Figure 6): only three models (from two modeling centers) show non-negligible trends bucking the dry consensus in West Africa in JJ, and only one bucks the wet consensus in Central-Eastern Africa in SO. Still, a JJ projection that ranges from 80% decline to 30% increase (and vice versa for SO) is far from a complete success.

One measure of progress from the CMIP3 archive is in the models' ability to simulate the right amplitude of the observed centennial trend (Figure 3.a), but can they also capture the magnitude of the decadal and multi-decadal variations? Figure 7 compares the distributions of 25-year, 50-year and 95-year trends in observations and in three sets of model integrations: the pre-industrial controls, the 20th century historical simulations, and the 21st century RCP8.5 projections (running windows over the available period in each integration were used to calculate the individual trends). In the top panels, we compare the observations to

the historical and control runs; the histograms are not normalized and are plotted on a semi-log scale to emphasize the low counts. The blue and gray lines to the left of each plot indicate the one-in-a-hundred trend in the simulations and help put the observed trends in context. The observations show a predominance of drying trends at all timescales. The observed centennial trends (Figure 7c) fall well within the distribution for the historical runs, an indication that the forced integrations can capture the observed magnitude quite well; instead, trends of the observed magnitude are rarer than one in a hundred in the absence of external forcings. At shorter timescales, the models underestimate the strength of the observed multi-decadal trends, so that strong drying trends are much more likely in the observations than in the model simulations for both the pre-industrial and the 20th century periods. In the bottom panels of Figure 7 we compare the distributions for the 20th and 21st century. At

the shortest time-scale of 25 years, the two are very similar, with only a slight preference for drying trends in the 20th century and wetting trends in the 21st. At longer timescales, the forced trends become more prominent and the two distributions diverge. The histogram for the 20th century simulations narrows, consistent with the expectation of more muted variability at the longest timescales, and becomes centered at around -5%, about a quarter of the observed 20th century trend. Conversely, the histograms for the projected 50- and 95-year trends spread out, reflecting model disagreement and increased uncertainty.

4. Pathways of CO₂ influence on the Sahel

The cause for disagreement in projections of total rainy season rainfall has been investigated at great depth in the context of the CMIP3 simulations, and it remains unclear. Attempts to discard or accept different projections based on the quality of the models' historical simulations [for example, *Cook and Vizy*, 2006; *Lau et al.*, 2005] have not been successful, consistent with similar experience in attempts to constrain climate sensitivity [for example, *Klocke et al.*, 2011] and with theoretical work [*Weigel et al.*, 2010]. Quite surprisingly, given how SST changes drove the 20th century Sahel rainfall changes, different trends in SST over the tropical Atlantic and Indo-Pacific oceans (or, equivalently, free-troposphere temperature in the tropics) cannot account for different trends in rainfall, at least not if we require that the same rainfall/SST relationship holds at inter-annual and centennial timescales [*Biasutti et al.*, 2008; *Caminade and Terray*, 2010]. While current work has proposed that the relative warming of the North Atlantic (with respect to the tropical mean) can explain more than a quarter of the intra-ensemble scatter (Alessandra Giannini, personal communication), several studies [*Patricola and Cook*, 2010; *Giannini*, 2010; *Skinner et al.*, 2012] have shown that the (fast) response of the land-atmosphere system to the local enhanced GHG forcing is as important as the (slow) response mediated through the warming of SST, and different sensitivities to each process should be considered in explaining the intra-ensemble differences in the projections.

Idealized simulations from the CMIP5 archive can perhaps help resolve this puzzle. In this section, we use three ensemble sets of idealized simulations (available only for a subset of CMIP5 models, see Fig. 9). In the first set (1%to4X), carbon dioxide concentration grows by 1% per year, doubling the pre-industrial value at year 70, quadrupling by year 140, and remaining constant thereafter; to the extent that short-lived species' influence on climate is weaker than that of CO₂, we expect the idealized coupled simulations to produce a climate similar to the scenario simulations. The second set of simulations (SSTclim4X) is uncoupled and is designed to extract the fast response of the atmosphere to CO₂ increase: we compare control simulations that are forced by pre-industrial climatological SST and pre-industrial CO₂ concentrations to experiments in which the CO₂ concentration is quadrupled, but SST is left unchanged. The third set (Abrupt4X) comprises coupled simulations in which the initial state is pre-industrial, but CO₂ concentration are held fixed at four times the pre-industrial value; trends in these simulation capture the slow climate response to CO₂, as the SST equilibrates to radiative forcing from the heightened CO₂ concentration.

Figure 8a compares the changes in rainfall in the 1%to4X simulations with those in the RCP8.5 simulations over the extended rainy season (May through October); each dot represents the linear trend over 140 and 95 years (for 1%to4X and RCP8.5, respectively) for a calendar month and CMIP5 model. In the aggregate, there is a clear linear relationship

between trends in these two sets of simulation, with small scatter, and with small departure from the 1:1 line. This is strong indication that other forcings in the scenario simulation are less important than the well-mixed greenhouse gases in setting the rainfall response in the Sahel.

Having established that the idealized simulation is a good stand in for the scenario simulation, we can try to decompose the full response of the coupled system to increasing CO₂ into two components: the fast, land-atmosphere response to increasing GHG concentrations and the slow response to the warming SST. Such linear decomposition is not achieved, as the fast and slow response do not add up to the full coupled response. This can be seen in two measures, shown in Figure 8b and Figure 9. Figure 8b compares the Sahel precipitation monthly trends in the 1%to4X simulations to the sum of the fast and slow response estimated from SST-clim4X and Abrupt4X simulations, respectively. The sum of the two components does not fall on the 1:1 line, instead, the full coupled response is much stronger than the sum of the fast and slow response and it does not vanish when the latter do (the linear fits for individual months or the full year do not go through the origin).

One would not necessarily expect a perfect correspondence, given the way the individual components of the response are estimated; specifically, uncoupled integrations can provide biased estimates of the coupled response [for example, *Douville*, 2005] and internal variability is likely to muddle our estimate of the response, especially in coupled integrations [for example, *Deser et al.*, 2010]. But even if we can accept both the departures from the identity line and the indifferent correlation, our impression that a linear decomposition is indeed problematic is supported by the annual cycle of the trends. These are shown in Figure 9 for the individual idealized simulations and for the sum of the fast and slow responses. When CO₂ increases are taken in isolation, with no attendant SST changes, the response is a robust wetting of the Sahel throughout the year, with positive anomalies peaking in August. This positive response is consistent with the importance of enhanced land-sea temperature contrast [*Haarsma et al.*, 2005] and enhanced energy input [*Giannini*, 2010] in boosting monsoon rainfall. When the response to SST warming is seen in isolation, the response is a robust drying of the Sahel that also persists throughout the year and peaks at the core of the rainy season, in August. This negative response is also consistent with some literature that has suggested remote drying outside of the main oceanic convective centers [*Neelin et al.*, 2003] due to the increased tropical stability that accompanies a uniform warming of the tropical oceans [*Held and Soden*, 2006]. All else equal, warmer and moister tropics would support enhanced precipitation, so the negative anomalies in the Sahel must be the result of dominant changes in the regional circulation and relative humidity.

Contrary to a presumption of linearity, is the fact that the CMIP5 ensemble suggests that these mechanisms interact in a complex way in the fully coupled system. The slow and fast response to CO₂ both peak in August, and their linear superposition shows moderate wetting throughout the rainy season. Thus, the seasonal signature of the trends in the 1%to4X (and RCP scenario) simulations—namely the fact that early season drying is turned around into a late season wetting of the Sahel—cannot be easily explained by the two mechanisms being dominant at different times of year. One caveat is that we do not have all the necessary idealized simulations to perform this decomposition on the entire CMIP5 ensemble. It would be a welcome development if, when more integrations become available, the current interpretation will be challenged and a simple linear superposition were to suffice as an explanation. The nature of the non-linear interaction between the fast and slow responses to CO₂ quadrupling is unclear, but we speculate that the mutual influences of land and ocean that are important in creating the observed annual cycle of surface temperature and precipitation [*Li and Philander*, 1997; *Fu et al.*, 2001; *Biasutti et al.*, 2003, 2005; *Dwyer et al.*, 2012] are also important in its modulation by increased greenhouse gases. This hypothesis is the focus of current research.

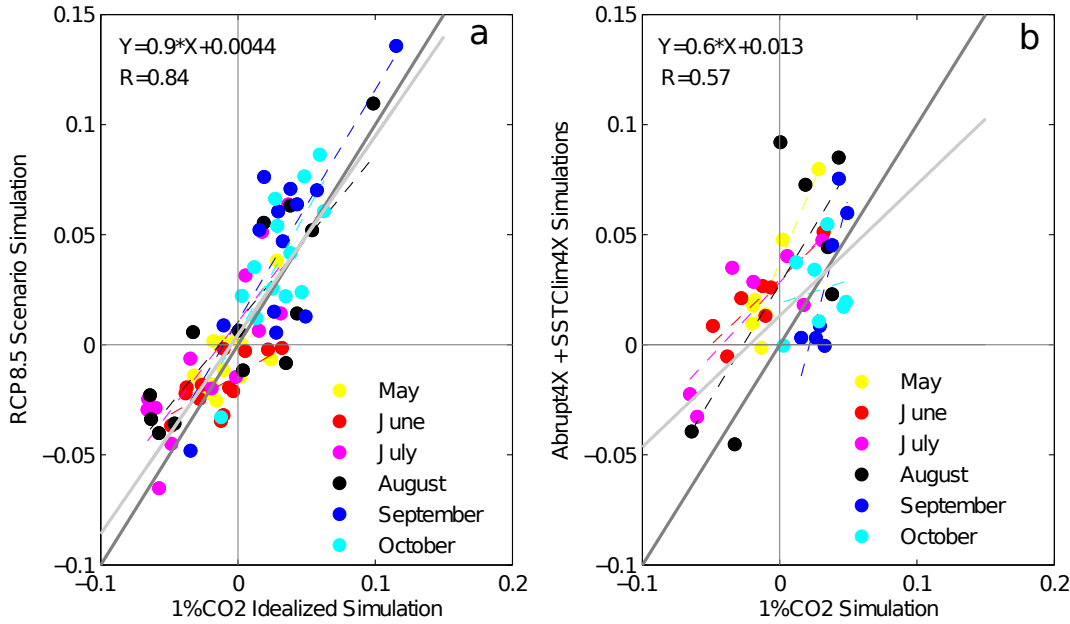


Figure 8. Comparison of rainy-season monthly Sahel rainfall changes in the 21st century and in idealized simulations forced by quadrupling CO₂. Left: Monthly trend in Sahel rainfall in the RCP8.5 scenario plotted against their counterparts in the 1%to4X idealized simulation. Right: The sum of the slow and fast responses to CO₂ (calculated as the long-term trends in the Abrupt4xCO₂ runs plus the difference between the SSTClim4xCO₂ and SSTClim runs), plotted against the trends in the coupled 1%to4X runs. Each dot represents one model and one calendar month. Colors indicate the calendar month for which the trends or anomalies are computed, as indicated by the legend. The dark grey line is the 1:1 line, while the light grey line is the best linear fit across all points. Linear fits for the individual months are also plotted as colored dashed lines. Units are in fraction of total rainfall.

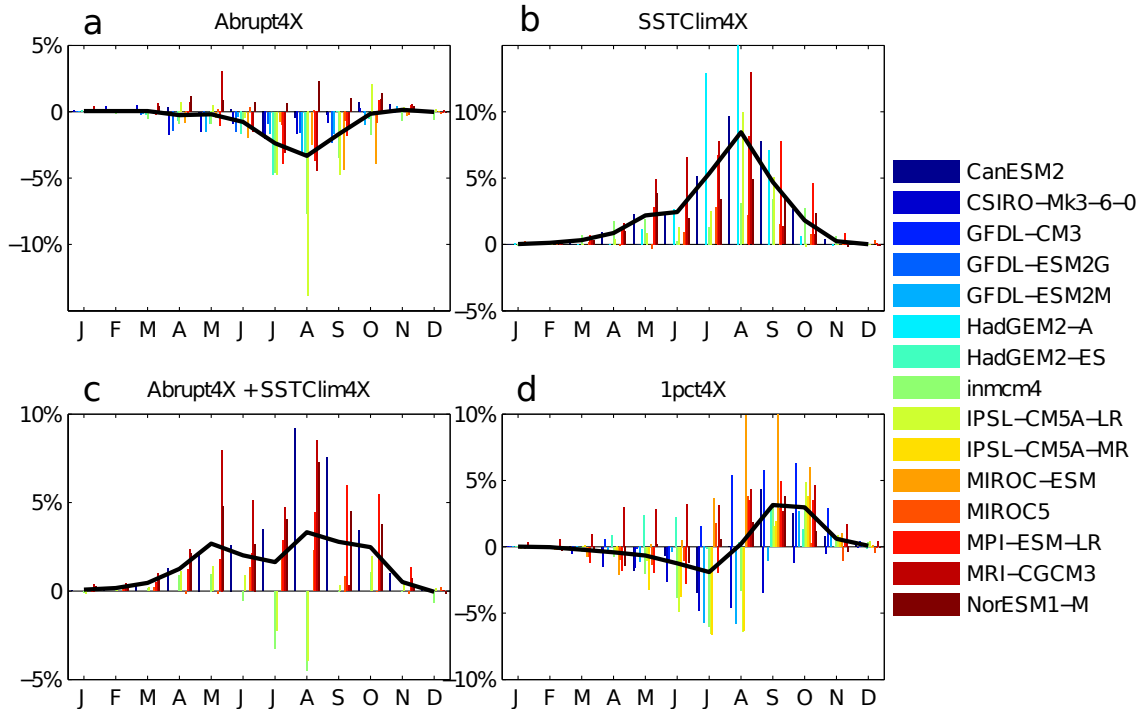


Figure 9. Annual cycle of Sahel rainfall changes in idealized runs capturing the fast and slow response to CO₂ and the combined effects. Top left: Anomalies due to SST (slow response) are calculated as long-term trends in the Abrupt4xCO₂ runs. Top right: Anomalies due to CO₂ (fast response) are calculated as the difference between the SSTClim4xCO₂ and SSTClim runs. Bottom left: the linear combined effect of CO₂ and SST is calculated as the sum of the top panels. Bottom right: the full effect of quadrupling CO₂ is calculated as the trend over 140 years integrations with CO₂ growing by 1% per year. Units are in percentage of total annual rainfall. Models are color coded as in the legend, but not all models are present in all panels.

questions of great consequence remain open. First: why do most models underestimate multi-decadal oscillations in Sahel rainfall? Second: what is the source of uncertainty in the projections?

Individual coupled simulations do reproduce the decadal ups and downs of the observed Sahel rainfall: Held *et al.* [2005] documented the case of one GFDL model, and we see the same for one MIROC model (not shown). But notwithstanding these good matches, the weak skewness of the simulated distributions (Figure 7), compared to the prevalence of strong multi-decadal drying trends in observations, suggests that something might still be missing in these models. Even setting aside the possibility that multi-decadal forcing from reflective and absorbing aerosols is underplayed, there is no shortage of candidates: from dust [Mahowald *et al.*, 2010], to vegetation [Kucharski *et al.*, 2012], to mesoscale organization of rainfall [Taylor *et al.*, 2011]. And some basic processes are obviously not properly represented in these models, as the CMIP5 models stubbornly retain the biases that have plagued previous-generation models in this region [Roehrig *et al.*, 2013]: from the absence of a cold tongue in the Gulf of Guinea, Richter and Xie [2008], to the misplacement of the Sahel rain band [Cook and Vizzy, 2006] and the African Easterly Jet [Ruti *et al.*, 2011], to the misrepresentation of African Easterly Waves [Ruti and Dell'Aquila, 2010]. Until we can trust that climate models capture the main structure of the regional climate and the full extent of variability in Sahel rainfall, a more quantitative attribution of past trends to anthropogenic forcings will remain elusive.

Even as the continuous presence of outlier models and the uncertainty regarding the magnitude of the projected anomalies remain troubling, the agreement across the CMIP5 models (four fifths of the models agree in sign) adds weight to the 21st century projections of a dryer onset season in West Africa and an intensification of the late rainy season throughout the Sahel. The 1%to4X idealized simulations of CMIP5 indicate that these projections are a response to increasing greenhouse gases, with no discernible role for aerosols and short-lived species.

The switch from dry to wet anomalies as the rainy season progresses has been described as part of a delay in the seasonal march of rainfall in the oceanic ITCZ and monsoon regions and has been linked to seasonal changes in SST [Biasutti and Sobel, 2009] and to the sensitivity of convective margins to changes in tropospheric stability [Lintner and Neelin, 2007; Seth *et al.*, 2010] and surface energy budget [Seth *et al.*, 2010; Giannini, 2010]. In light of our results, these arguments will have to be refined. Idealized simulations designed to distinguish the direct effect of enhanced greenhouse gases concentration (the fast response) and the indirect effect mediated through changes in SST (the slow response) show that each effect changes Sahel rainfall in opposite ways throughout the rainy season, but that the two effects do not add up to a delay of the rains (in the models available for this analysis). We do not doubt that the above-mentioned mechanisms play a role in setting the Sahel anomalies, but we caution that local radiation and remote SST seem to interact in a complex way. We speculate that the mutual influences of land and ocean, and the inherent difference in the phase and amplitude of their annual cycle, are important in determining the projected delay of the Sahel rains in the coupled response.

Acknowledgments. We acknowledge the World Climate Research Programme's Working Group on Coupled Modelling, which is responsible for CMIP, and we thank the climate modeling groups for producing and making available their model output. For CMIP the U.S. Department of Energy's Program for Climate Model Diagnosis and Intercomparison provides coordinating support and led development of software infrastructure in partnership with the Global Organization for Earth System Science Portals

Many heartfelt thanks to Haibo Liu and Naomi Naik for acquiring the datasets and making them easy to work

with. This work was supported in part by NOAA (RAPID-NA08OAR4320754), and by NSF (SES-1048946).

References

- Ackerley, D., B. B. Booth, S. H. E. Knight, E. J. Highwood, D. J. Frame, M. R. Allen, and D. P. Rowell, Sensitivity of Twentieth-Century Sahel Rainfall to Sulfate Aerosol and CO₂ Forcing, *Journal of Climate*, *24*, 4999–5014, 2011.
- Biasutti, M., Atmospheric science: A man-made drought, *Nature Climate Change*, *1*, 197–198, 2011.
- Biasutti, M., and A. Giannini, Robust Sahel drying in response to late 20th century forcings., *Geophys. Res. Lett.*, *33*, L11,706, 2006.
- Biasutti, M., and A. Sobel, Delayed seasonal cycle and African monsoon in a warmer climate, *Geophys. Res. Lett.*, *36*, L23,707, 2009, doi:10.1029/2009GL041303.
- Biasutti, M., D. S. Battisti, and E. S. Sarachik, The annual cycle over the tropical Atlantic, South America, and Africa, *J. Climate*, *16*, 2491–2508, 2003.
- Biasutti, M., D. S. Battisti, and E. S. Sarachik, Terrestrial influence on the annual cycle of the Atlantic ITCZ., *J. Climate*, *18*, 211–228, 2005.
- Biasutti, M., I. M. Held, A. H. Sobel, and A. Giannini, SST forcings and Sahel rainfall variability in simulations of the twentieth and twenty-first centuries, *Journal of Climate*, *21*, 3471–3486, 2008.
- Biasutti, M., A. H. Sobel, and S. J. Camargo, The role of the Sahara Low in summertime Sahel rainfall variability and change in the CMIP3 models., *Journal of Climate*, *22*, 5755–5771, 2009.
- Booth, B. B. B., N. J. Dunstone, P. R. Halloran, T. Andrews, and N. Bellouin, Aerosols implicated as a prime driver of twentieth-century North Atlantic climate variability, *Nature*, *484*, 228–232, 2012.
- Brooks, G. E., Climate and History in West Africa, in *Transformations in Africa: Essays on Africa's Later Past*, edited by G. Connah, pp. 139–159, University Press, London - Washington, 1998.
- Caminade, C., and L. Terray, Twentieth century Sahel rainfall variability as simulated by the ARPEGE AGCM, and future changes, *Climate Dynamics*, *35*, 75–94, 2010.
- Cook, K., and E. K. Vizzy, Coupled model simulations of the West African monsoon system: 20th and 21st century simulations., *J. Climate*, *19*, 3681–3703, 2006.
- Deser, C., A. Phillips, V. Bourdette, and H. Teng, Uncertainty in climate change projections: the role of internal variability, *Climate Dynamics*, 2010.
- Douville, H., Limitations of time-slice experiments for predicting regional climate change over South Asia, *Climate Dynamics*, *24*, 373–391, 2005.
- Dwyer, J. G., M. Biasutti, and A. H. Sobel, Projected Changes in the Seasonal Cycle of Surface Temperature, *Journal of Climate*, *25*, 6359–6374, 2012.
- Evan, A., Climate science: Aerosols and Atlantic aberrations, *Nature*, *484*, 170–171, 2012.
- Friedlingstein, P., et al., Climate-carbon cycle feedback analysis: Results from the C4MIP model intercomparison, *Journal of Climate*, *19*, 3337–3353, 2006.
- Fu, R., R. E. Dickinson, M. Chen, and H. Wang, How do tropical sea surface temperatures influence the seasonal distribution of precipitation in the equatorial Amazon?, *J. Climate*, *14*, 4003–4026, 2001.
- Giannini, A., Mechanisms of Climate Change in the Semiarid African Sahel: The Local View, *Journal of Climate*, *23*, 743–756, 2010.
- Giannini, A., R. Saravanan, and P. Chang, Oceanic forcing of Sahel rainfall on interannual to interdecadal time scale, *Science*, *302*, 1027–1030, 2003.
- Haarsma, R. J., F. M. Selden, S. L. Weber, and M. Kliphuis, Sahel rainfall variability and response to greenhouse warming., *Geophys. Res. Lett.*, *32*, L17,702, 2005.

- Hagos, S., and K. Cook, Ocean warming and late-twentieth-century Sahel drought and recovery, *Journal of Climate*, *21*, 3797–3814, 2008.
- Held, I. M., and B. J. Soden, Robust response of the hydrological cycle to global warming, *J. Climate*, *19*, 5686–5699, 2006.
- Held, I. M., T. L. Delworth, J. Lu, K. L. Findell, and T. R. Knutson, Simulation of Sahel drought in the 20th and 21st centuries., *Proc. Natl. Acad. Sci.*, *102*, 17,891–17,896, 2005.
- Hoerling, M., J. Hurrell, J. Eischeid, and A. Phillips, Detection and attribution of 20th century northern and southern African rainfall change., *J. Climate*, *19*, 3989–4008, 2006.
- Hulme, M., A 1951-80 global land precipitation climatology for the evaluation of general circulation models, *Climate Dyn.*, *7*, 57–72, 1992.
- Joly, M., A. Voldoire, H. Douville, P. Terray, and J.-F. Royer, African monsoon teleconnections with tropical SSTs: validation and evolution in a set of IPCC4 simulations, *Climate Dynamics*, *29*, 1–20, 2007.
- Klocke, D., R. Pincus, and J. Quaas, On Constraining Estimates of Climate Sensitivity with Present-Day Observations through Model Weighting, *Journal of Climate*, *24*, 6092–6099, 2011.
- Kucharski, F., N. Zeng, and E. Kalnay, A further assessment of vegetation feedback on decadal Sahel rainfall variability, *Climate Dynamics*, 2012.
- Lau, K. M., S. S. P. Shen, K.-M. Kim, , and H. Wang, A multimodel study of the twentieth-century simulations of Sahel drought from the 1970s to 1990s, *J. Geophys. Res.*, *111*, 2005.
- Levy II, H., M. D. Schwarzkopf, L. Horowitz, V. Ramaswamy, and K. L. Findell, Strong sensitivity of late 21st century climate to projected changes in short-lived air pollutants, *Journal of Geophysical Research*, *113*, D06,102, 2008.
- Levy II, H., L. W. Horowitz, M. D. Schwarzkopf, Y. Ming, J.-C. Golaz, V. Naik, and V. Ramaswamy, The Roles of Aerosol Direct and Indirect Effects in Past and Future Climate, *Journal of Geophysical Research*, Submitted, 1–46, 2012.
- Li, T., and S. G. H. Philander, On the seasonal cycle of the equatorial Atlantic, *J. Climate*, *10*, 813–817, 1997.
- Lintner, B. R., and J. Neelin, A prototype for convective margin shifts, *Geophysical Research Letters*, *34*, L05,812, 2007.
- Mahowald, N. M., et al., Observed 20th century desert dust variability: impact on climate and biogeochemistry, *Atmospheric Chemistry and Physics*, *10*, 10,875–10,893, 2010.
- Mitchell, T., and P. Jones, An improved method of constructing a database of monthly climate observations and associated high-resolution grids, *International journal of climatology*, *25*, 693–712, 2005.
- Mohino, E., S. Janicot, and J. Bader, Sahel rainfall and decadal to multi-decadal sea surface temperature variability, *Climate Dynamics*, *37*, 419–440, 2011.
- Neelin, J. D., C. Chou, and H. Su, Tropical drought regions in global warming and El Niño teleconnections., *Geophys. Res. Lett.*, *30*, 2275, 2003.
- Nicholson, S., Climatic Variations in the Sahel and Other African Regions During the Past Five Centuries , *Journal of Arid Environments*, *1*, 3–24, 1978.
- Nicholson, S. E., B. Some, and B. Kone, An analysis of recent rainfall conditions in West Africa, including the rainy seasons of the 1997 El Niño and the 1998 La Niña years, *J. Climate*, *13*, 2628–2640, 2000.
- Patricola, C. M., and K. Cook, Sub-Saharan Northern African climate at the end of the twenty-first century: forcing factors and climate change processes, *Climate Dynamics*, *37*, 1165–1188, 2010.
- Peterson, T. C., and R. S. Vose, An Overview of the Global Historical Climatology Network Temperature Database, *Bulletin of the American Meteorological Society*, *78*, 2837–2849, 1997.
- Power, S. B., F. Delage, R. Colman, and A. Moise, Consensus on Twenty-First-Century Rainfall Projections in Climate Models More Widespread than Previously Thought, *Journal of Climate*, *25*, 3792–3809, 2012.
- Riahi, K., S. Rao, V. Krey, C. Cho, V. Chirkov, G. Fischer, G. Kindermann, N. Nakicenovic, and P. Rafaj, RCP 8.5—A scenario of comparatively high greenhouse gas emissions, *Climate Change*, *109*, 33–57, 2011.
- Richter, I., and S.-P. Xie, On the origin of equatorial Atlantic biases in coupled general circulation models, *Climate Dynamics*, *31*, 587–598, 2008.
- Roehrig, R., D. Bouniol, F. Guichard, F. Hourdin, and J. L. Redelsperger, The present and future of the West African monsoon: a process-oriented assessment of CMIP5 simulations along the AMMA transect. , *Journal of Climate*, pp. 1–88, 2013.
- Ruti, P., et al., The west african climate system: a review of the amma model inter-comparison initiatives, *Atmospheric Science Letters*, *12*, 116–122, 2011.
- Ruti, P. M., and A. Dell’Aquila, The twentieth century African easterly waves in reanalysis systems and IPCC simulations, from intra-seasonal to inter-annual variability, *Climate Dynamics*, *35*, 1099–1117, 2010.
- Scaife, A. A., et al., The CLIVAR C20C project: selected twentieth century climate events, *Clim Dyn*, 2008.
- Seth, A., S. A. Rauscher, M. Rojas, A. Giannini, and S. J. Camargo, Enhanced spring convective barrier for monsoons in a warmer world?, *Climatic Change Letters*, 2010, accepted.
- Shanahan, T. M., J. T. Overpeck, K. J. Anchukaitis, J. W. Beck, J. E. Cole, D. L. Dettman, J. A. Peck, C. A. Scholz, and J. W. King, Atlantic Forcing of Persistent Drought in West Africa, *Science*, *324*, 377–380, 2009.
- Skinner, C. B., M. Ashfaq, and N. S. Diffenbaugh, Influence of Twenty-First-Century Atmospheric and Sea Surface Temperature Forcing on West African Climate, *Journal of Climate*, *25*, 527–542, 2012.
- Stevens, B., and G. Feingold, Untangling aerosol effects on clouds and precipitation in a buffered system, *Nature*, *461*, 607–613, 2009.
- Taylor, C. M., A. Gounou, F. Guichard, P. P. Harris, R. J. Ellis, F. Couvreur, and M. De Kauwe, Frequency of Sahelian storm initiation enhanced over mesoscale soil-moisture patterns, *Nature Geoscience*, *4*, 430–433, 2011.
- Taylor, K. E., R. J. Stouffer, and G. A. Meehl, An Overview of CMIP5 and the Experiment Design, *Bulletin of the American Meteorological Society*, *93*, 485–498, 2012.
- Ting, M., Y. Kushnir, R. Seager, and C. Li, Forced and Internal Twentieth-Century SST Trends in the North Atlantic, *Journal of Climate*, *22*, 1469–1481, 2009.
- Weigel, A. P., R. Knutti, M. A. Liniger, and C. Appenzeller, Risks of Model Weighting in Multimodel Climate Projections, *Journal of Climate*, *23*, 4175–4191, 2010.
- Yoshioka, M., N. M. Mahowald, A. J. Conley, W. D. Collins, D. W. Fillmore, C. S. Zender, and D. B. Coleman, Impact of Desert Dust Radiative Forcing on Sahel Precipitation: Relative Importance of Dust Compared to Sea Surface Temperature Variations, Vegetation Changes, and Greenhouse Gas Warming, *Journal of Climate*, *20*, 1445–1467, 2007.
- Zeng, N., J. D. Neelin, K.-M. Lau, and C. J. Tucker, Enhancement of interdecadal climate variability in the Sahel by vegetation interaction, *Science*, *286*, 1537–1540, 1999.
- Zhang, C., P. Woodworth, and G. Gu, The seasonal cycle in the lower troposphere over west africa from sounding observations., *Q. J. R. Meteorol. Soc.*, *132*, 2561–2584, 2006.

M. Biasutti, Lamont-Doherty Earth Observatory of Columbia University. 61 Route 9W. Palisades, NY 10964-8000 (biasutti@ldeo.columbia.edu)